An electric detection of immunoglobulin G in the enzyme-linked immunosorbent assay using an indium oxide nanoparticle ion-sensitive field-effect transistor

J. Micromech. Microeng. **22** (2012) 015009 (9pp) doi:10.1088/0960-1317/22/1/015009

An electric detection of immunoglobulin G in the enzyme-linked immunosorbent assay using an indium oxide nanoparticle ion-sensitive field-effect transistor

Dongjin Lee[1] **and Tianhong Cui**[2]

Department of Mechanical Engineering, University of Minnesota, 111 Church Street Southeast, Minneapolis, MN 55455, USA

E-mail: tcui@me.umn.edu

Received 15 April 2011, in final form 1 October 2011
Published 20 December 2011
Online at stacks.iop.org/JMM/22/015009

Abstract

Semiconducting nanoparticle ion-sensitive field-effect transistors (ISFETs) are used to detect immunoglobulin G (IgG) in the conventional enzyme-linked immunosorbent assay (ELISA). Indium oxide and silica nanoparticles were layer-by-layer self-assembled with the oppositely charged polyelectrolyte as the electrochemical transducer and antibody immobilization site, respectively. The assay was conducted on a novel platform of indium oxide nanoparticle ISFETs, where the electric signals are generated in response to the concentration of target IgG using the labeled detecting antibody. The sandwiched ELISA structure catalyzed the conversion of the acidic substrate into neutral substance with the aid of horseradish peroxidase. The pH change in the substrate solution was detected by nanoparticle ISFETs. Normal rabbit IgG was used as a model antigen whose detection limit of 0.04 ng ml^{-1} was found. The facile electric detection in the conventional assay through the semiconducting nanoparticle ISFET has potential applications as a point-of-care detection or a sensing element in a lab-on-a-chip system.

(Some figures in this article are in colour only in the electronic version)

1. Introduction

Immunosensors are analytical devices to yield the measurable signal that is sensitive and selective to the specific protein by means of the antigen–antibody interaction. They carry out direct monitoring of a molecular recognition event and diagnosis of pathogen. The sensitivity and detection limit of immunosensors should be optimized for a target molecule or pathogen of interest. Each protein has its own 'normal' reference range inside the body. For example, prostate-specific antigen, a secreted cancer biomarker, has the normal serum level of a few ng ml^{-1} that increases several hundred times when the cancer develops [1]. In the case of interleukin-6, an oral cancer marker, the normal concentration is nearly 1000 times lower than prostate-specific antigen, leading to the detection challenge [2]. Despite the excellent sensitivity of clinical methods such as enzyme-linked immunosorbent assay (ELISA), fluorescent and chemiluminescent immunoassays, radioimmunoassay and electrophoretic immunoassay, they are offset by the necessity of expensive equipment and laborious sample preparation. Hence, a simple, sensitive, reliable and inexpensive diagnostic method is highly desired along with miniaturization without affecting the sensitivity or detection limit.

The bioassay should yield the detectable signal that is proportional to the concentration of proteins of interest. One of the most widely used detection methods is the spectrophotometric assay where the absorption of light at a particular wavelength corresponds to a concentration of the target molecule. Nonetheless, it is disadvantageous due to

[1] Current address: Department of Mechanical Engineering, Korea Advanced Institute of Science and Technology, 291 Daehak-ro, Yuseong-gu, Daejeon 305-701, Korea.

[2] Author to whom any correspondence should be addressed.

the interference from other chromophores and the necessity of laboratory equipment. Instead of conventional detection mechanisms such as mass [3], heat [4], electrochemistry [5–7] and optics [8–10], an ion-sensitive field-effect transistor (ISFET) based on semiconducting nanoparticle thin-film is demonstrated as a novel detection platform this work.

Nanomaterial-based biosensors have attracted much attention due to low cost as the off-the-shelf building blocks and extraordinary properties. Quantum dot labeled electrochemical immunosensors demonstrated a detection range of 0.1–10 ng ml^{-1} with a detection limit of 30 pg ml^{-1} immunoglobulin G (IgG) using voltammetry response [11]. Zirconia nanoparticles and ZnS@CdS quantum dots were used for construction of phosphorylated acetylcholinesterase as a biomarker of organophosphate pesticides [12]. However, the nanoparticles have been used only as immobilization sites or labels to detect immuno-reaction or catalyze electrochemical reaction. Combined with advantages of electrochemistry such as a sensitive miniaturized measurement system, excellent pH-sensitive electrical conductance was found in nanomaterial thin-film [13, 14], which augments the application to immunosensors [15].

The electric detection of IgG in the ELISA is demonstrated in this work by exploiting a semiconducting nanoparticle thin-film ISFET on which the conventional ELISA was conducted. The nanoparticle thin-film was hierarchically composed of indium oxide and silica nanoparticles as an electrochemical transducer and antibody immobilization site. Through the ISFET characterization scheme the electric detection was performed in the formulated substrate solution in which pH of substrate solution changed. Horseradish peroxidase (HRP) enzyme conjugated on the detecting antibody catalyzed the reaction that resulted in pH shift. Subsequently, the pH change was detected by ISFET sensors. The electric detection through the nanoparticle ISFET in the conventional assay demonstrated a detection limit of 0.04 ng ml^{-1} for the normal rabbit IgG. The autonomous assay could be developed using the nanoparticle ISFET detection method in combination with microfludics and/or lab-on-a-chip system.

2. Experimental details

2.1. Materials and reagents

Goat anti-rabbit IgG F(ab′)$_2$ (sc-3836) and normal rabbit IgG (sc-2027) were purchased from Santa Cruz Biotechnology. Mouse anti-rabbit IgG conjugated with HRP (AP188P) was from Chemicon. Goat anti-rabbit IgG labeled with Alexa Fluor® 488 was obtained from Invitrogen. Antibodies were diluted into 1× phosphate buffered saline (PBS, GIBCO) or 3% (w/v) bovine serum albumin (BSA) blocking buffer (Fraction V Solution 7.5%, Invitrogen) in 1× PBS. The received goat anti-rabbit IgG F(ab′)$_2$ was diluted 500-fold to produce a concentration of 0.8 μg ml^{-1}. Normal rabbit IgG was diluted to 3% (w/v) BSA in PBS to yield serial concentrations of 0.04, 0.4, 4, 40 and 400 ng ml^{-1}. Mouse anti-rabbit IgG-HRP was diluted 2000-fold resulting in a concentration of 0.4 μg ml^{-1}. Ascorbic acid and o-phenylenediamine were purchased from Sigma-Aldrich in order to formulate a substrate solution. The phosphate buffer at pH 6 with the buffer strength of 5 mM was prepared along with 15 mM NaCl. Subsequently, ascorbic acid and o-phenylenediamine were added to yield a concentration of 1 mM, respectively. The Indium oxide nanoparticle (INP) was purchased from Sigma-Aldrich, and the colloidal silica nanoparticle (SNP, SNOWTEX®-XL) was from Nissan Chemical America Corp. INPs were dispersed into 0.12 mM of HCl (pH 3.9) to generate a positively charged surface with a concentration of 50 mg ml^{-1}. An as-received colloidal SNP of 4 g was diluted to 100 mL of deionized water (DIH$_2$O) resulting in a concentration of 16 mg ml^{-1}. Polydiallyldimethylammonium chloride (PDDA, M_w = 200–350 k), polystylenesulfonate (PSS, M_w = 70 k) and poly-L-lysine (PLL, 0.1 wt%) were obtained from Sigma-Aldrich. The aqueous concentration of PDDA and PSS used for layer-by-layer self-assembly was 1.4 wt% and 0.3 wt%, respectively, with 0.5 M sodium chloride (NaCl). PLL was used as received.

2.2. Nanoparticle thin-film ISFET fabrication

The fabrication procedure is schematized in figure 1. The left column represents the semiconducting sensing site, while the right column depicts the elongated measuring pads for electrical connection. Chromium (25 nm) and gold (100 nm) were evaporated on the Si/SiO$_2$ wafer (figure 1(*a*)). The source and drain electrodes were patterned by photolithography (figure 1(*b*)). To block the unwanted reaction on the area other than the sensing channel, 200 cycles of aluminum oxide were deposited by atomic layer deposition (Savannah, Cambridge NanoTech). With the patterned layer of photoresist (Shipley S1813), an opening window was made on the sensing site and measuring pads as a result of etching in 1:10 buffered oxide etch (figure 1(*c*)). Photolithography was carried out to make photoresist lift-off mask for layer-by-layer assembled nanoparticle film (figure 1(*d*)). Nanoparticles were assembled in a sequence of [(PDDA, 10 min)/(PSS, 10 min)]$_3$ + [(INP, 15 min)/(PSS, 10 min)]$_5$ + [(PDDA, 10 min)/(PSS, 10 min)] + [(PDDA, 10 min)/(SNP, 4 min)]$_6$ (figure 1(*e*)) with intermediate washing and drying with nitrogen stream after assembly of each species. This assembly sequence produced about 28 nm of (INP/PSS) and 30 nm of (PDDA/SNP) bi-layers [16]. Finally, the silicon wafer was dipped into 0.1 wt% of PLL for an hour and lifted off using acetone, methanol and isopropyl alcohol, followed by the rinsing with DIH$_2$O (figure 1(*f*)).

2.3. Characterization

2.3.1. Fluorescence microscopy. Fluorescence microscopy was used to study PLL assembly and the immobilization of goat anti-rabbit IgG F(ab′)$_2$. For the PLL assembly study, an aqueous solution of PLL labeled with fluorophore (PLL-FAM) was used to optimize assembly time. Glass cover slips were treated with piranha solution (H_2SO_4:H_2O_2 3:1) at 120 °C for 20 min, followed by thorough rinsing with a copious amount of DIH$_2$O. Six layers of PDDA/SNP were assembled on the glass cover slips to mimic the outermost

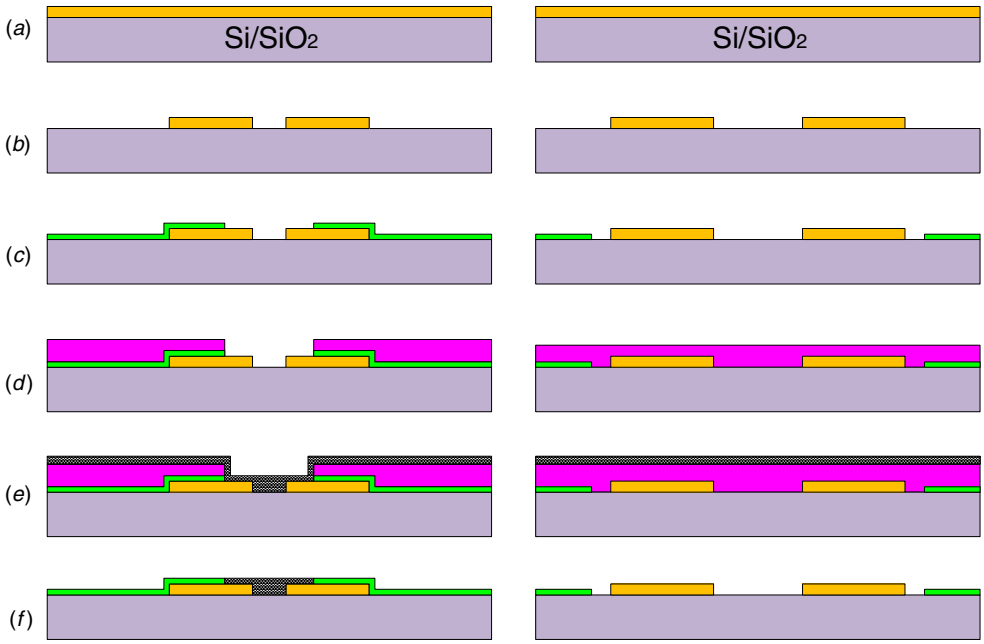

Figure 1. Fabrication process of layer-by-layer assembled semiconducting nanoparticle ISFET sensors (left: sensing site, right: measuring pads): (*a*) e-beam evaporation of chromium and gold, (*b*) metal patterning for source and drain electrodes, (*c*) patterning of aluminum oxide layer for passivation, (*d*) patterning of photoresist lift-off mask, (*e*) self-assembly of nanoparticles and (*f*) lift-off.

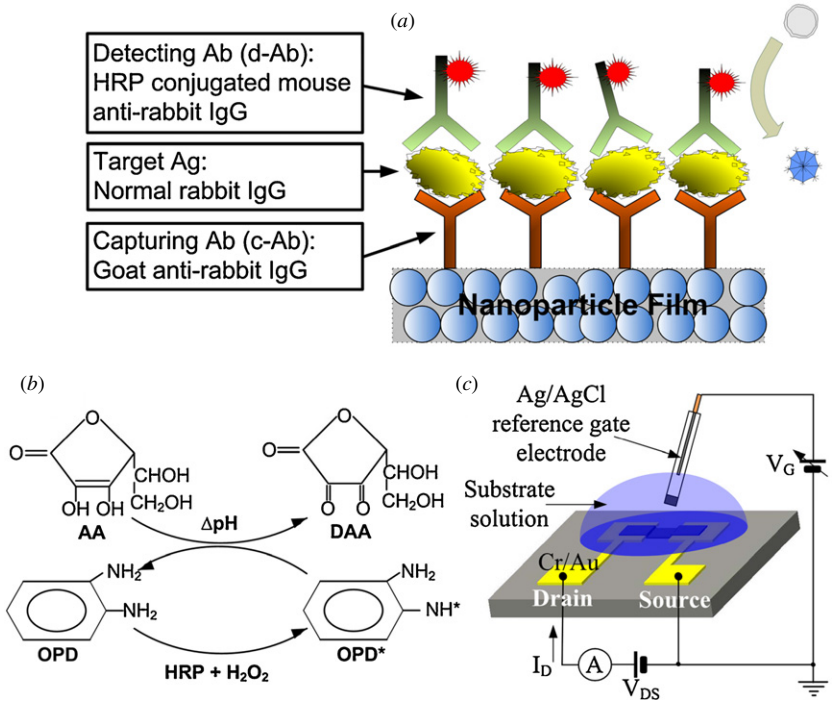

Figure 2. Scheme of the electric immunoassay in the pH-sensitive nanoparticle thin-film ISFET: (*a*) the sandwiched enzyme-linked immunosorbent assay (ELISA), (*b*) catalytic reaction of HRP for ascorbic acid (AA) and o-phenylenediamine (OPD) substrate system and (*c*) ISFET characterization scheme. The pH change in the substrate solution by the HRP catalytic function is detected by the INP ISFET.

layer of the nanoparticle thin-film platform. Then, they were incubated in 0.01 wt% aqueous PLL-FAM solution for 10, 30, 60 and 180 min. The control was incubated in DIH_2O for 180 min. Fluorescent images were obtained using a fluorescence microscope (Nikon, Eclipse TE200) with the blue excitation and green detecting filters at the same gain and exposure time. Fluorescence microscopy was also used in order to demonstrate the immobilization of goat anti-rabbit IgG $F(ab')_2$ on the PLL treated surface. To verify the binding, photoresist was patterned onto the glass slide (1 cm × 1 cm), followed by O_2 plasma treatment to change the surface hydrophilic. The patterned glass slide was incubated in

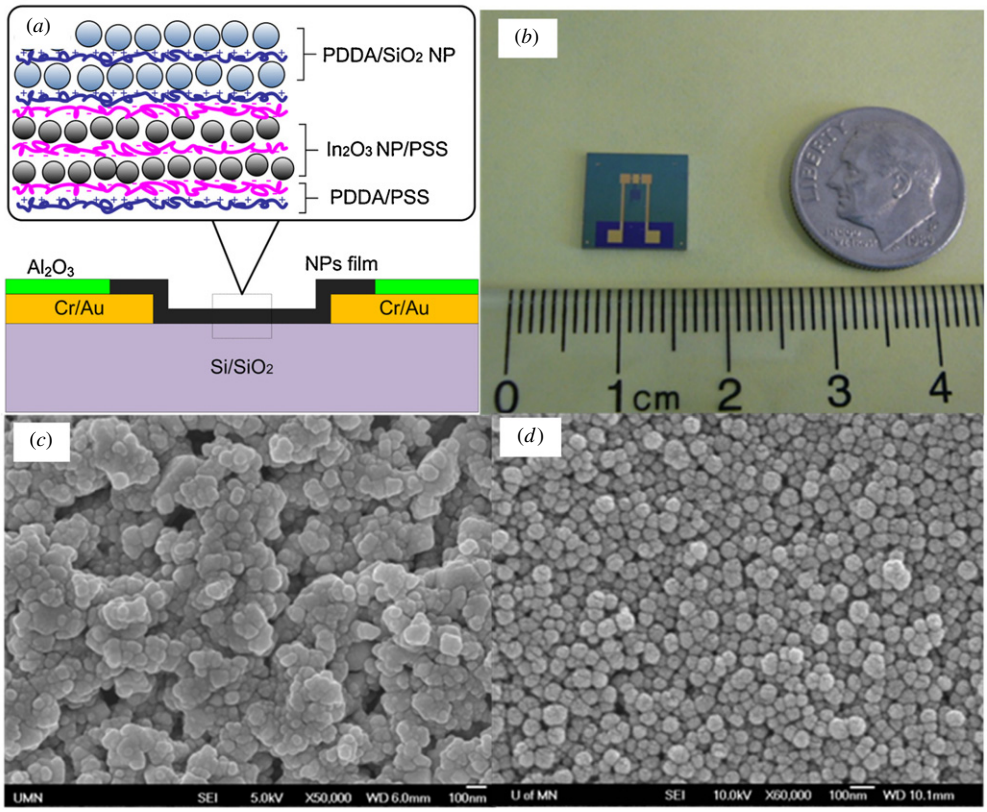

Figure 3. Fabricated nanoparticle ISFET: (*a*) cross-sectional device schematic with a thin-film architecture, (*b*) image of an individual device, SEM images of (*c*) INP terminated surface as an electrochemical transducer and (*d*) SNP terminated surface as an antibody immobilization site.

0.1 wt% PLL aqueous solution for an hour. Goat anti-rabbit IgG conjugated with Alexa Fluor® 488 was assembled on the slide overnight in a concentration of 1 μg ml^{-1} at 4 °C. Finally, photoresist was lifted off using acetone, methanol and isopropyl alcohol followed by the rinse with PBS. Fluorescent images were obtained before and after the lift-off of photoresist to compare the green intensity at the same gain and exposure time.

2.3.2. Contact angle measurement. The silicon wafer (2.5 cm × 2.5 cm) was treated in piranha solution, followed by the assembly of a nanoparticle multilayer in the aforementioned manner. A silicon substrate was incubated in 0.1 wt% PLL aqueous solution for 1 h. The static water contact angles were obtained using a contact angle measurement system (OCA-15, Data Physics) on 12 spots and averaged. The sessile contact angle was determined by placing a drop of water (5 μl) with a speed of 1 μl s^{-1} on the surface and recording the angle between the horizontal plane and the tangent to the drop at the point of contact with the substrate.

2.3.3. ELISA protocol and electrical characterization. The diced individual devices were sorted into 24-well plates for the ELISA. The immunoassay adopted in this study is detailed as follows:

(a) incubate ISFET devices in a goat anti-rabbit IgG solution with the concentration of 0.8 μg ml^{-1} overnight at 4 °C;
(b) rinse chips with 1× PBS three times using a shaker for 5 min each time;
(c) incubate chips in 3% (w/v) BSA blocking buffers at room temperature for 3 h to prevent the nonspecific binding, followed by rinsing as in step (b)
(d) incubate chips in a normal rabbit IgG solution with concentrations of 0.04, 0.4, 4, 40, 400 ng ml^{-1} for 1 h, followed by rinsing as in step (b);
(e) incubate chips in HRP conjugated mouse anti-rabbit IgG with the concentration of 0.4 μg ml^{-1} for an hour, followed by rinsing as in step (b).

Hydrogen peroxide of 0.3% (w/v) in water was mixed with ascorbic acid and o-phenylenediamine substrate solution with a volume ratio of 1:30 before use. The formulated substrate solution of 300 μl was applied on the ISFET that was incubated for 5 min for HRP-catalyzed reaction to occur. The ISFET characterization scheme was applied through a semiconductor parameter analyzer (HP4156B). The drain-to-source voltage (V_{DS}) was fixed at 1.0 V and the gate voltage (V_G) was scanned from 0 to −5 V with a step of 50 mV for all ISFETs prepared with various IgG concentrations.

3. Results and discussion

The electrochemical property of the self-assembled semiconducting INP and dielectric SNP thin-film was exploited in this work. The nanoparticle thin-film platform

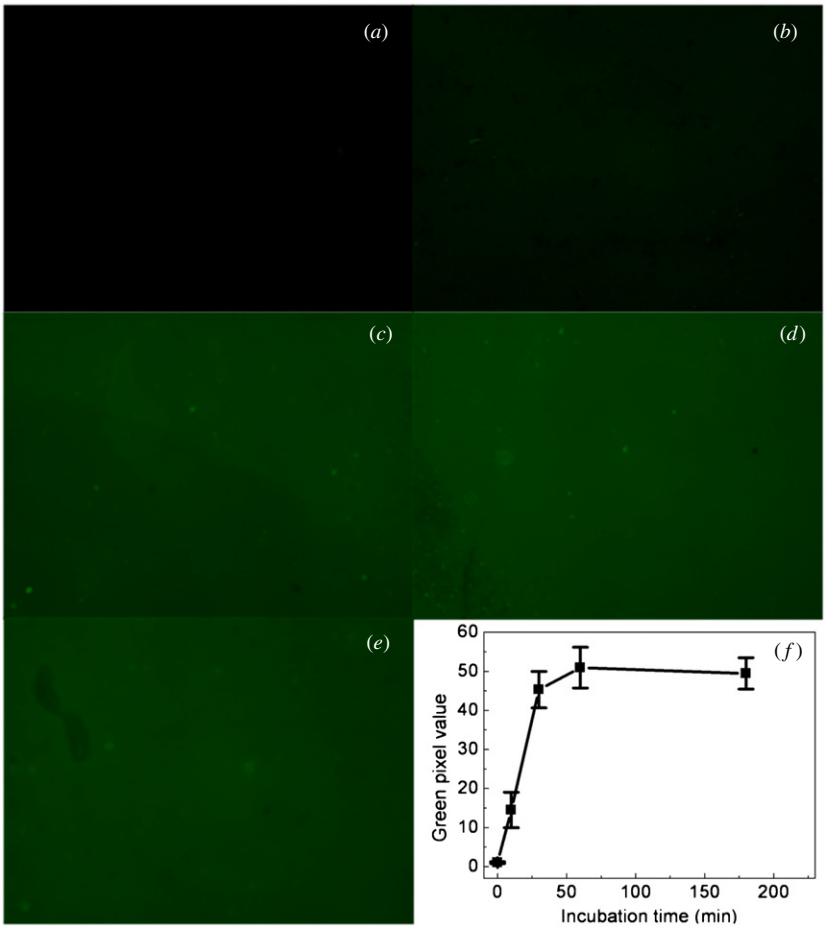

Figure 4. Fluorescent image of the PLL-FAM covered glass cover slip at various incubation times—the saturation time of 60 min is observed: (*a*) control sample dipped into DIH_2O for 3 h, the sample incubated in 0.01 wt% PLL-FAM for 10 (*b*), 30 (*c*), 60 (*d*), 180 min (*e*), and green pixel values (*f*) extracted the images from images (*a*)–(*e*) as a function of the incubation time: error bars in (*f*) indicate the standard deviation of all green pixel values.

employs the sandwiched ELISA structure as shown in figure 2(*a*). The capturing antibody (c-Ab, goat anti-rabbit IgG) was immobilized on the outmost SNP layer treated with PLL, and target antigen (normal rabbit IgG) was assembled onto c-Ab by the immuno-reaction. The detecting antibody (d-Ab, mouse anti-rabbit IgG) conjugated with HRP enzyme was used in order to produce the HRP-catalyzed substrate conversion as shown in figure 2(*b*), leading to the pH change. The catalytic cycle of HRP has been widely known, and a variety of substrate systems were studied using conventional ISFET systems [17]. The oxidation of ascorbic acid leads to the formation of dehydroascorbic acid, which gives the pH increase in the vicinity of HRP enzyme. The hydrogen ions produced here either diffuse away to the bulk solution or penetrate into nanoparticle film. Once the reaction reaches the steady state, the concentration profile could be determined. In addition, it was reported that pH shift made in oxidation of ascorbic acid by HRP could be amplified by adding o-phenylenediamine as an electron mediator [17]. The pH change corresponds to the amount of d-Ab labeled with HRP, which is dependent, in turn, on the amount of IgG bound on target antigen by means of the immuno-reaction. Consequently, the concentration of IgG in a sample can be traced by measuring the pH change using a nanoparticle thin-film ISFET as shown in figure 2(*c*). The miniaturized Ag/AgCl reference electrode with the internal filling solution of 3 M KCl was used along with the source and drain electrodes fabricated on the chip surface. The thin-film devices with sandwich structures made at various concentrations of IgG were tested in the formulated substrate solution.

The electrical conductance of nanoparticle thin-film in response to pH distribution comes from protonation/deprotonation of hydroxyl groups on the nanoparticle surface. The pH distribution leads to the change of protonation/deprotonation on both INPs and SNPs. The protonation status on the INP surface determines the conductance of thin-film by the space-charge model [18]. The pH decrease corresponds to less negative charges on the surface that makes the space-charge layer thinner, resulting in a reduced inter-particle Schottky barrier. On the other hand, the protonation status on the SNP surface comes into play in applying gate voltage in a sense of a field-effect transistor [14], where the pH decrease corresponds to the positive shift in gate voltage, which accumulates the conducting electrons in the underlying p-type INP layer. This dual effect influences the conductance

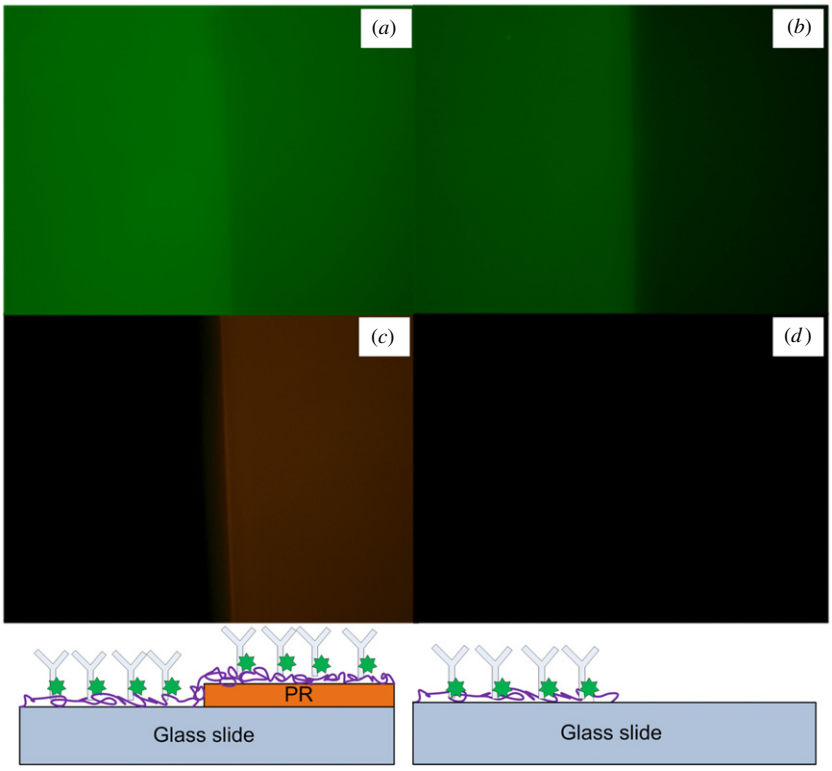

Figure 5. Fluorescence images of immobilized goat anti-rabbit IgG labeled with Alexa Fluor® 488 on patterned glass slides for c-Ab immobilization test: images (*a*) and (*c*) were obtained in the presence of photoresist, as shown in the schematic below, with the green and red detecting filter, respectively. Images (*b*) and (*d*) were taken after the lift-off of photoresist with the green and red detecting filter, respectively. The contrast image in (*b*) indicates that c-Ab is successfully immobilized on the SNP film through electrostatic interaction with PLL.

of nanoparticle thin-film, where the pH decrease results in more current.

This immunoassay features in three aspects: (1) exploitation of developed all-nanoparticle ISFET sensors [13] as a detection platform in the conventional assay, (2) enzyme-based signal amplification for pH shift and (3) HRP-catalyzed substrate–substrate activation. Furthermore, it is noticed that secondary antibodies were used as c-Ab and d-Ab, and the primary antibody as a model antigen for the demonstration of device functionality. This functionality can be extended to the detection of pathogen using primary antibody labeled with enzyme for the diagnostic purpose. In addition, pH-sensitive electrochemical properties of INP thin-film stimulate development of electrochemical immunosensors without electroactive metal ions. Instead, semiconducting INP thin-film is the active transducing element that converts the chemical information to electrical signal, while SNPs play a role of the immobilization sites of the ELISA structure.

The fabricated ISFET is shown in figure 3. The schematic of cross-section with the internal structure of nanoparticle thin-film is shown in figure 3(*a*), where the protective alumina is used for the passivation of biomolecular adsorption and electrochemical reaction in areas other than the semiconducting channel. The individual ISFET device used for the detection of IgG in this study has the size 1 cm × 1 cm, as shown in figure 3(*b*), with semiconducting channel dimensions of 10 μm in length and 1 mm in width. The SEM images of INP- and SNP-terminated surfaces are shown in figures 3(*c*) and (*d*), respectively.

A successful immunosensor is based on the stable interface of the capturing antibody with the sensor surface. Instead of covalent conjugation of antibodies on the surface using cross-linker carbodiimide such as 1-ethyl-3-(3-dimethylaminopropyl)carbodiimide (EDC), a simple electrostatic physisorption was employed to immobilize the antibody by using PLL. Hence, fluorescence microscopy was used to study PLL assembly onto the outmost SNP film and the immobilization of the capturing antibody on PLL. The fluorescent images of glass cover slips are shown in figures 4(*a*)–(*e*) with different dipping times of 0, 10, 30, 60 and 180 min in the aqueous solution of PLL labeled with fluorescent dye (PLL-FAM). The control sample was made in pure water and is considered 0 min incubation time. Apparently, the green intensity increases with the dipping time, and it becomes saturated at the dipping time of 60 min. No green signal was found in the control sample, which was dipped in DIH_2O for 3 h. The green pixel values were extracted and averaged over the whole image. The averaged green pixel values over the image are illustrated in figure 4(*f*) as a function of the dipping time. The error bars indicate the standard deviation.

The fluorescent images of the immobilized goat anti-rabbit IgG labeled with Alexa Fluor® 488 are illustrated in figure 5. The left column images, figures 5(*a*) and (*c*), were obtained in the glass slides with the photoresist pattern as

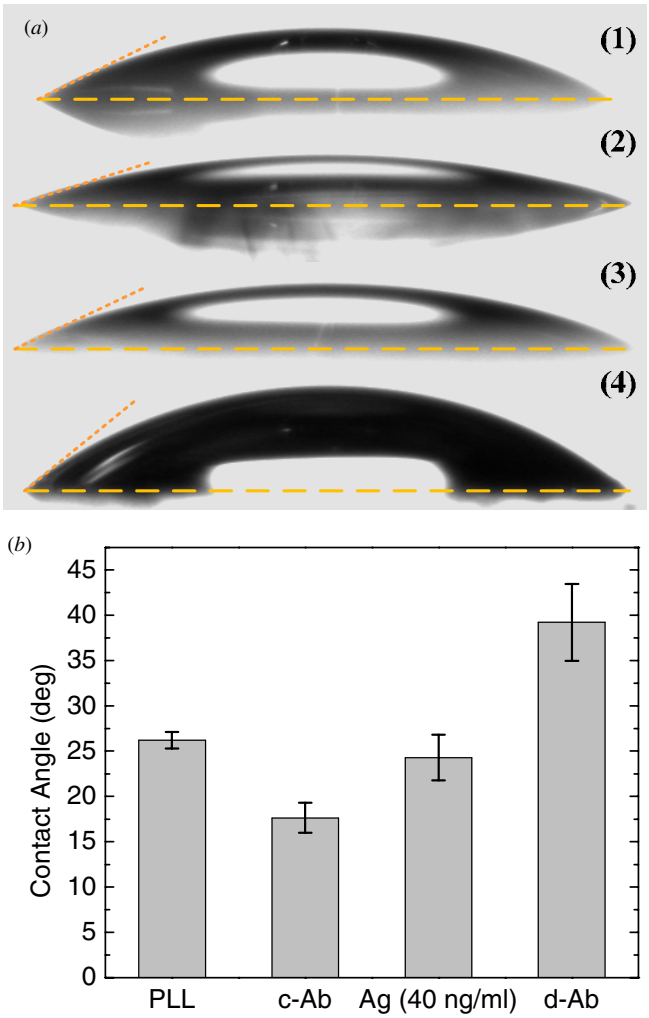

Figure 6. Static water contact angle measurement in the ELISA process: (*a*) sessile water drop images at the surface of PLL (1), goat anti-rabbit IgG (2), normal rabbit IgG (3) in the case of 40 ng ml^{-1} concentration used, and HRP labeled mouse anti-rabbit IgG (4) and (*b*) contact angle measurement at each step of the ELISA.

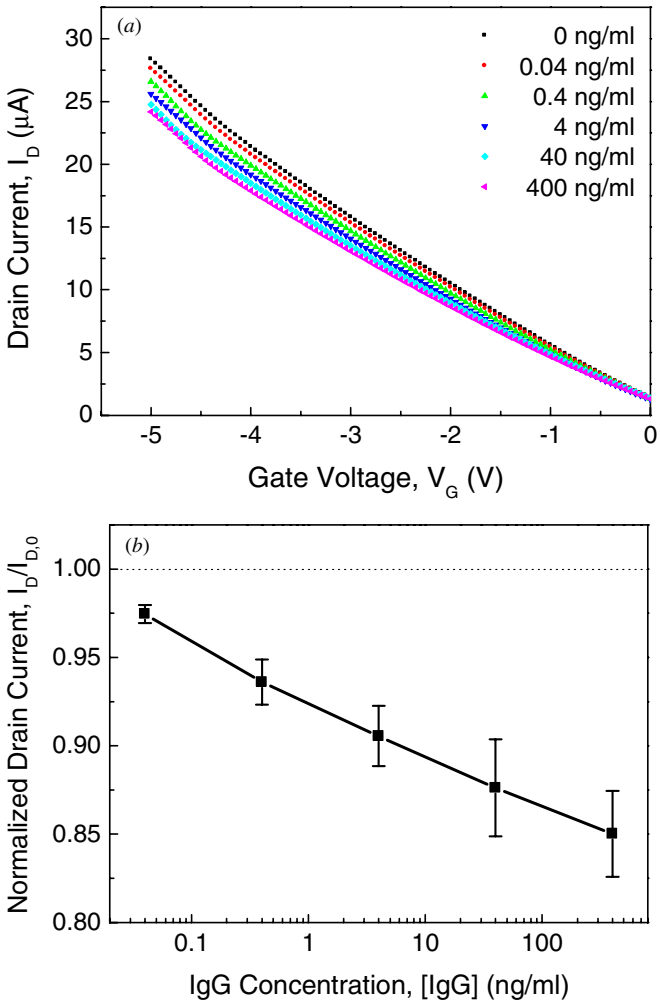

Figure 7. Electric detection of IgG concentration using the ISFET characterization scheme: (*a*) typical drain current (I_D) versus gate voltage (V_G) while drain to source voltage (V_{DS}) was kept at 1.0 V, and (*b*) normalized drain currents (I_D) with respect to the current at 0 ng ml^{-1} concentration versus IgG concentration at the gate voltage of −5.0 V. The different transconductance is observed in image (*a*) due to the pH change in the substrate solution. The error bars in image (*b*) indicate standard deviation. The dotted line in image (*b*) demonstrates the background signal, which was obtained at 0 ng ml^{-1} concentration of IgG. The detection of 0.04 ng ml^{-1} is obtained clearly.

shown in the schematics below. The blue and green excitation filters with green and red detection filters, respectively, were used for figures 5(*a*) and (*c*). On the other hand, the right column images, figures 5(*b*) and (*d*), were taken after the lift-off of the photoresist. The same combination of excitation and detection filters was used for figures 5(*b*) and (*d*), as in figures 5(*a*) and (*c*), respectively. It is apparent to observe green light all over the surface in figure 5(*a*), since c-Ab was immobilized on the photoresist as well as on the glass surface. Once the photoresist was removed the green light became dark resulting in the contrast image as in image (*b*), which means that c-Ab was removed from the photoresist surface, while it still remained on the glass surface. It seemed that the red component in image (*c*) originated from the existence of photoresist that was disappeared in image (*d*). Therefore, images (*c*) and (*d*) confirm that photoresist was entirely removed from the surface. It is concluded that the capturing antibodies are successfully immobilized on the PLL treated glass surface.

Complementary to fluorescence microscopy, the static water contact angle was measured to readily verify the changes on the surface in each step of the ELISA. If there are any changes in the surface energy from the chemical [19] component and topographical changes [20] on the surface, the water contact angle changes. The contact angle measurement is a good tool to characterize immobilized proteins [21]. The result of the static contact angle measurement is shown in figure 6. The representative sessile water droplet images at the surface of PLL (1), goat anti-rabbit IgG (2), normal rabbit IgG (3) bound in the concentration of 40 ng ml^{-1} and HRP-labeled mouse anti-rabbit IgG (4) are illustrated in figure 6(*a*). The corresponding contact angles are depicted in figure 6(*b*), where the abrupt decrease in the contact angle upon c-Ab

immobilization and the gradual increase upon Ag and d-Ab binding are observed.

The result of ISFET characterization at various IgG concentrations is shown in figure 7. Typical drain currents versus the gate voltage from a set of ELISA are depicted in figure 7(*a*). As the gate voltage increases negatively, the conductance of the channel also increases in all the devices tested. However, it is observed that the transconductance increases with the decrease in IgG concentration. The amount of IgG determines the amount of d-Ab as a kind of signal amplification scheme. More HRPs catalyze the breakdown of more ascorbic acid leading to a greater pH increase. pH sensitivity found in the INP ISFET tells that the conductivity decreases with the increase in pH, which is in good agreement with the reported result [13]. The currents were normalized with the current at the IgG concentration of 0 ng ml^{-1} and the gate voltage of −5.0 V. The normalized currents were replotted as a function of IgG concentration as shown in figure 7(*b*). The error bars indicate the standard deviation from multiple sets of ELISA. It is noticeable that the linear response to pH in the acidic region [13] enables us to obtain the linear response per decade in the range of IgG concentrations tested, which is promising in the immunosensor development. The dotted lines represent the electric current from the ISFET made as control in 3% (w/v) BSA solution without any IgGs included. Therefore, the current at 0 ng ml^{-1} IgG concentration qualitatively reflects the nonspecific binding of d-Ab and the leakage current in the ISFET itself. We used this electric current as a background signal, so that the detection limit of the electric immunoassay using nanoparticles was found as 0.04 ng ml^{-1}, which corresponds to 0.26 pM and 1.56×10^8 IgGs ml^{-1} based on IgG's molecular weight of 155 kDa. The electric IgG immunosensor through the nanoparticle thin-film ISFET exhibited a wider detection range and 10-fold smaller detection limit than other reported CNT-based IgG sensors [15, 22, 23] presumably due to two kinds of signal amplification schemes and direct electric detection in the nanoparticle layer.

4. Conclusion

The nanoparticle thin-film ISFET has been used as the electric detection platform in the ELISA. The antibodies were immobilized on the SNP effectively with the aid of PLL polyelectrolyte as demonstrated in fluorescence microscopy presumably due to the biocompatibility and size similarity. The detecting antibody labeled with HRP exploited the chain reaction between ascorbic acid and o-phenylenediamine to accelerate and amplify the pH change, which could be detected by the underlying semiconducting nanoparticle thin-film ISFET. As a model antigen, normal rabbit IgG was detected with the detection limit of 0.04 ng ml^{-1}. It is not necessary to use bench-top instruments to acquire observable signals. Furthermore, it could be more miniaturized and combined with microfluidic systems to perform the elegant analytical assays. The nanoparticle thin-film ISFET detection platform suggests novel and delicate analytical devices eliminating the need of sophisticated bench-top instrumentation and tedious sample preparation.

Acknowledgments

The authors would like to thank Professor Andy Taten at the Department of Chemistry, University of Minnesota for providing PLL-FAM. This work was supported in part by the Defense Advanced Research Projects Agency (DARPA) N/MEMS S&T Fundamentals program under grant no HR001-06-1-0500 issued to the Micro/nano Fluidics Fundamentals Focus (MF3) Center. Part of the work was carried out at the Nanofabrication Center and Characterization Facility at the University of Minnesota, which receives partial support from NSF through the NNIN program.

References

[1] Okuno J, Maehashi K, Kerman K, Takamura Y, Matsumoto K and Tamiya E 2007 Label-free immunosensor for prostate-specific antigen based on single-walled carbon nanotube array-modified microelectrodes *Biosens. Bioelectron.* **22** 2377–81

[2] Malhotra R, Patel V, Vaque J P, Gutkind J S and Rusling J F 2010 Ultrasensitive electrochemical immunosensor for oral cancer biomarker IL-6 using carbon nanotube forest electrodes and multilabel amplification *Anal. Chem.* **82** 3118–23

[3] Vaughan R D, O'Sullivan C K and Guilbault G G 2001 Development of a quartz crystal microbalance (QCM) immunosensor for the detection of Listeria monocytogenes *Enzyme Microb. Technol.* **29** 635–8

[4] Pizziconi V B and Page D L 1997 A cell-based immunobiosensor with engineered molecular recognition: part I. Design feasibility *Biosens. Bioelectron.* **12** 287–99

[5] Sklaal P 1997 Advances in electrochemical immunosensors *Electroanalysis* **9** 737–45

[6] Sadik O A and Van Emon J M 1996 Applications of electrochemical immunosensors to environmental monitoring *Biosens. Bioelectron.* **11** i–x

[7] Plekhanova Y V, Reshetilov A N, Yazynina E V, Zherdev A V and Dzantiev B B 2003 A new assay format for electrochemical immunosensors: polyelectrolyte-based separation on membrane carriers combined with detection of peroxidase activity by pH-sensitive field-effect transistor *Biosens. Bioelectron.* **19** 109–14

[8] Marks R, Margalit A, Bychenko A, Bassis E, Porat N and Dagan R 2000 Development of a chemiluminescent optical fiber immunosensor to detect Streptococcus pneumoniae antipolysaccharide antibodies *Appl. Biochem. Biotechnol.* **89** 117–26

[9] Kubitschko S, Spinke J, Brükner T, Pohl S and Oranth N 1997 Sensitivity enhancement of optical immunosensors with nanoparticles *Anal. Biochem.* **253** 112–22

[10] Duendorfer J and Kunz R E 1998 Compact integrated optical immunosensor using replicated chirped grating coupler sensor chips *Appl. Opt.* **37** 1890–4

[11] Liu G, Lin Y-Y, Wang J, Wu H, Wai C M and Lin Y 2007 Disposable electrochemical immunosensor diagnosis device based on nanoparticle probe and immunochromatographic strip *Anal. Chem.* **79** 7644–53

[12] Liu G, Wang J, Barry R, Petersen C, Timchalk C, Gassman P and Lin Y 2008 Nanoparticle-based electrochemical immunosensor for the detection of phosphorylated acetylcholinesterase: an exposure biomarker of organophosphate pesticides and nerve agents *Chem.—Eur. J.* **14** 9951–9

[13] Liu Y and Cui T 2007 Ion-sensitive field-effect transistor based pH sensors using nano self-assembled

polyelectrolyte/nanoparticle multilayer films *Sensors Actuators* B **123** 148–52
[14] Lee D and Cui T 2009 pH-dependent conductance behaviors of layer-by-layer self-assembled carboxylated carbon nanotube multilayer thin-film sensors *J. Vac. Sci. Technol.* B **27** 842–8
[15] Lu M, Lee D, Xue W and Cui T 2009 Flexible and disposable immunosensors based on layer-by-layer self-assembled carbon nanotubes and biomolecules *Sensors Actuators* A **150** 280–5
[16] Cui T, Liu Y and Zhu M 2005 Field-effect transistors with layer-by-layer self-assembled nanoparticle thin films as channel and gate dielectric *Appl. Phys. Lett.* **87** 183105
[17] Akimenko V K, Khomutov S M, Obraztsova A Y, Vishnivetskii S A, Chuvilskaya N A, Laurinavichus K S and Reshetilov A N 1996 A rapid method for detection of Clostridium thermocellum by field-effect transistor-based immunodetection *J. Microbiol. Methods* **24** 203–9
[18] Franke M E, Koplin T J and Simon U 2006 Metal and metal oxide nanoparticles in chemiresistors: does the nanoscale matter? *Small* **2** 36–50
[19] Janssen D, De Palma R, Verlaak S, Heremans P and Dehaen W 2006 Static solvent contact angle measurements, surface free energy and wettability determination of various self-assembled monolayers on silicon dioxide *Thin Solid Films* **515** 1433–8
[20] Kim P, Kim D H, Kim B, Choi S K, Lee S H, Khademhosseini A, Langer R and Suh K Y 2005 Fabrication of nanostructures of polyethylene glycol for applications to protein adsorption and cell adhesion *Nanotechnology* **16** 2420
[21] Stadler H, Mondon M and Ziegler C 2003 Protein adsorption on surfaces: dynamic contact-angle (DCA) and quartz-crystal microbalance (QCM) measurements *Anal. Bioanal. Chem.* **375** 53–61
[22] Cid C C, Riu J, Maroto A and Rius F X 2008 Carbon nanotube field effect transistors for the fast and selective detection of human immunoglobulin G *Analyst* **133** 1005–8
[23] Fermandez-Sanchez C, Pellicer E, Orozco J, Jimenez-Jorquera C, Lechuga L M and Mendoza E 2009 Plasma-activated multi-walled carbon nanotube-polystyrene composite substrates for biosensing *Nanotechnology* **20** 335501